LANGMUIR Article
Cite This: Langmuir 2019, 35, 14712−14724
pubs.acs.org/Langmuir

Hydrogen-Bonded Multilayer Thin Films and Capsules Based on Poly(2-*n*-propyl-2-oxazoline) and Tannic Acid: Investigation on Intermolecular Forces, Stability, and Permeability

Nirmal Mathivanan,[†,‡] Gokul Paramasivam,[†,‡] Maarten Vergaelen,[§] Jayakumar Rajendran,[†,‡] Richard Hoogenboom,[*,§] and Anandhakumar Sundaramurthy[*,†,‡]

[†]SRM Research Institute and [‡]Department of Physics and Nanotechnology, SRM Institute of Science and Technology, Kattankulathur, 603203 Kanchipuram, Tamil Nadu, India

[§]Supramolecular Chemistry Group, Department of Organic and Macromolecular Chemistry, Ghent University, Krijgslaan 281 S4, B-9000 Ghent, Belgium

Supporting Information

ABSTRACT: In recent years, hydrogen-bonded multilayer thin films and capsules based on neutral and nontoxic building blocks have been receiving interest for the design of stimuli-responsive drug delivery systems and for the preparation of thin-film coatings. Capsule systems made of tannic acid (TA), a natural polyphenol, as a hydrogen bonding donor and poly(2-*n*-propyl-2-oxazoline) (PnPropOx), a polymer with lower critical solution temperature around 25 °C, as a hydrogen bonding acceptor are advantageous over other conventional hydrogen-bonded systems because of their high stability in physiological pH range, biocompatibility, good renal clearance, stealth behavior, and stimuli responsiveness for temperature and pH. In this work, investigations on the interactive forces in TA/PnPropOx capsule formation, film thickness, stability, and permeability are reported. The multilayer thin films were assembled on quartz substrates, and the layer-by-layer film growth was investigated by UV−vis spectroscopy, atomic force microscopy, and profilometry. Hollow capsules were fabricated by sequential coating of TA and PnPropOx onto $CaCO_3$ colloidal particles, followed by template dissolution with a 0.2 M ethylenediaminetetraacetic acid solution. The obtained capsules and multilayer thin films were found to be stable over a wide pH range of 2−9. It is found that both hydrogen bonding and hydrophobic interactions are responsible for the enhanced stability of the capsules at higher pH range. Swelling followed by dissolution of the capsules was observed at a pH value lower than 2, while the capsules undergo shrinking at a pH value higher than 8 and finally transform into a particle-like morphology before dissolution. The TA/PnPropOx capsules reported here could be used as a temperature-responsive drug delivery system in controlled drug delivery applications.

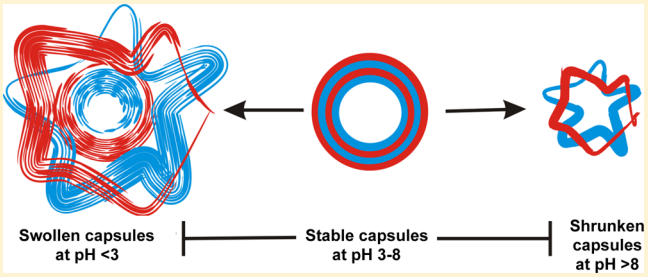

1. INTRODUCTION

Stimuli-responsive hollow polymeric capsules fabricated via layer-by-layer (LbL) assembly are of great interest for biomedical applications, as encapsulated biologically active molecules or drugs are protected in a confined space with micro- or nanoscale dimensions by a thin permeable shell.[1−5] The permeability of the shell can be manipulated using a variety of different types of interactions, such as electrostatic interactions, hydrogen bonding, host−guest interactions, hydrophobic interactions, and charge-transfer halogen interactions.[6−9] Such capsules, with in-built responsiveness against environmental (e.g., pH, ionic strength, polarity, and temperature) and external triggers (e.g., magnetic field, electric current, ultrasound, and laser light), enable a definite control on the transport of a defined quantity of drugs or other biologically active molecules across the capsule membrane in ways that are not possible with conventional systems. The protective shell can be used for both triggering the release of loaded molecules and extending the time of release, while protecting the load from external stress up to the delivery stage.[10−12] Thus, these capsules can be used for a large variety of applications, ranging from nanoreactors and microcages to study chemical reactions, to sensors for nanomedicine, and to drug delivery for the diagnosis and treatment of diseases.[13−16] However, issues of cytotoxicity with the use of polycations in electrostatically assembled capsules, and questions regarding the stability of hydrogen-bonded capsules at physiological conditions, limit their use in practical applications.

In recent years, hydrogen-bonded hollow capsules made from neutral and nontoxic building blocks, especially with tannic acid (TA) and poly(2-alkyl-2-oxazoline)s (PAOx) as the hydrogen bond donor and acceptor, respectively, have

Received: September 18, 2019
Revised: October 17, 2019
Published: October 17, 2019

DOI: 10.1021/acs.langmuir.9b02938
Langmuir 2019, 35, 14712−14724

Scheme 1. Chemical Structures of (a) PnPropOx, (b) Carboxyfluorescein, (c) Tannic Acid, (d) Rhodamine 6G, (e) Tetramethylrhodamine Isothiocyanate-Dextran (TRITC-Dextran), and (f) Fluorescein Isothiocyanate-Dextran (FITC-Dextran)

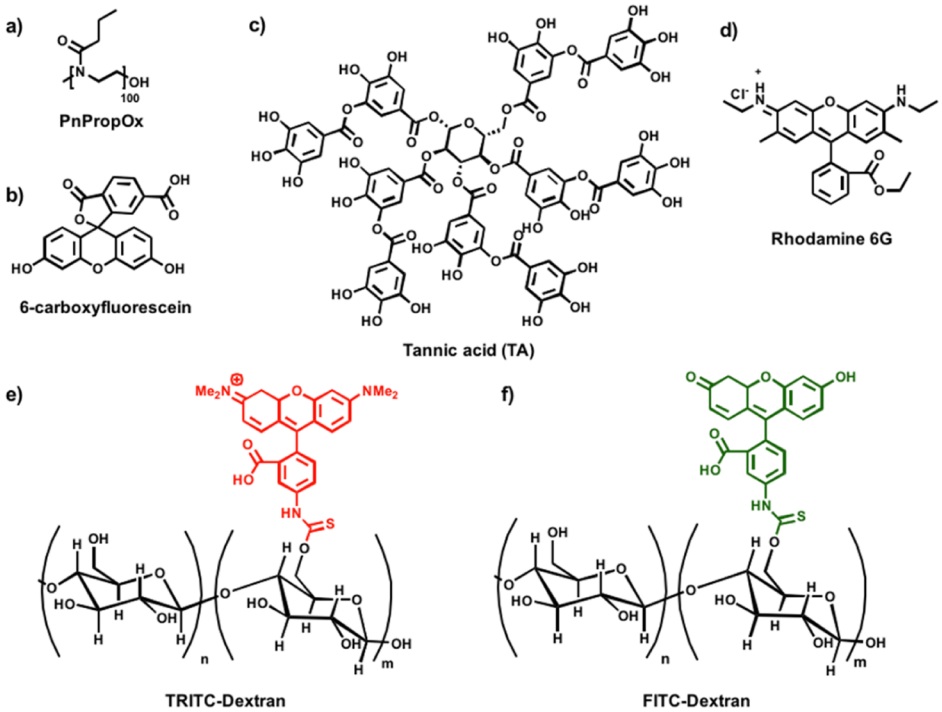

emerged as a promising stimuli-responsive system.[17−19] There are many advantages in using TA/PAOx system for drug delivery applications. First, the absence of cations prevents the cytotoxicity-related issues. Second, the use of a natural multibranched polyphenol, TA, may provide stable hydrogen-bonded capsules at physiological conditions without the need for a post-modification process such as carbodiimide chemistry and photo- or thermo-induced cross-linking methods.[20−22] The drawback of post-modification processes is that the stability of the film at physiological conditions has a negative impact on the stimuli responsiveness of the capsule shell.[20,21,23] In addition to the above-mentioned advantages of polyphenols, TA is known to exhibit inhibitory effects on membrane lipid peroxidation and decrease the risk of tumor formation, inflammation, and bacterial and viral infections.[24,25] Studies on the biological and chemical properties of PAOx polymers have proven their high physical and chemical stability, stealth behavior, antifouling characteristics, and good renal clearance.[26−28] In addition, they provide options for easy and direct access to surface functionalization of capsules for targeted delivery either by post-modification of the chain ends or introducing functional moieties in the side chains via copolymerization of functional 2-oxazoline monomers.[29−32]

Many attempts have been made to fabricate multilayer thin films on both planar substrates and colloidal templates using TA and PAOx with different alkyl side chains that result from the 2-substituent of the corresponding 2-oxazoline monomers. The nature of the side chains of PAOx and its cloud point temperature as well as the assembly parameters such as temperature and pH play an important role in the growth, thickness, permeability, and morphology of the LbL-assembled films. However, based on the hydrophilic or hydrophobic nature of the side chains, the film growth is controlled by either enthalpy or entropy.[19] Although PAOx interacts with TA via hydrogen bonding, the permeability of thin films and capsules can be easily controlled by manipulating the configuration of the polymers via changing the temperature. Furthermore, the dynamic nature of the hydrogen bonds and the high mobility of the polymer chains at the film−water interface can be used in self-repairing the accidental damage of the assembled films.[33] Alternatively, Chapman et al. reported that poly(2-ethyl-2-oxazoline) (PEtOx) conjugates with cyclic octapeptides form nanotubes in water that are reversibly transformed into microparticles, when the suspension temperature is increased above the T_{CP}.[34] As PEtOx is known to exhibit a slow transition around its T_{CP}, the formed nanotubes slowly reorganize themselves into hydrophobic microparticles and precipitate from the solution. Hendessi et al. reported the synthesis of Ag nanoparticles (NPs) using PEtOx as a stabilizing agent, which is used to fabricate the multilayers of Ag NPs and TA.[35] The film growth follows a linear regime which is stable up to pH 8.5 similar to control PEtOx/TA multilayer films. Hollow capsules made of PMA and different forms of PEtOx (e.g., linear form, brushlike form, and thiol-containing PEtOx) have also been reported by the LbL assembly process. It is noteworthy that stable capsules were only obtained after cross-linking the layer components.[12,36]

Among all the reported PAOx−capsule systems, the poly(2-*n*-propyl-2-oxazoline) (PnPropOx)/TA system results in interesting thermoresponsive capsules for drug delivery applications as the capsule permeability can be switched between closed and open states at a physiological temperature of 37 °C.[7] When drug-loaded capsules are heated to 37 °C, the PnPropOx chains in the capsule shell undergo a morphological transformation from linear chain form into aggregated polymer globules, which triggers the release of loaded cargo molecules.[18,19] An investigation of poly(2-isopropyl-2-oxazoline) (PIPOX))/TA multilayer thin films for encapsulation and

DOI: 10.1021/acs.langmuir.9b02938
Langmuir 2019, 35, 14712−14724

release of doxorubicin (Dox), by Haktaniyan et al., shows that the release is higher at acidic pH ranges as protonation of TA disrupts the electrostatic interactions between TA and Dox.[37] At an intermediate pH range, TA undergoes deprotonation that results in a stronger electrostatic interaction with Dox, and hence, the release is lower at physiological temperature.[37,38]

Recently, we have reported a proof-of-concept study on stable TA/PnPropOx hollow capsules without any cross-linking of the layer components (i.e., capsules retain its responsiveness) using $CaCO_3$ microparticles as sacrificial templates and demonstrated that TA/PnPropOx capsules undergo a morphological transformation upon heating to physiological temperature, leading to release of loaded molecules of different sizes.[7] Previous reports on the interaction between 4-fluorophenol and tertiary amides as well as PAOx and water show that the interactions are purely based on the hydrogen bonds between the carbonyl groups of the amides and the phenyl groups of TA.[18,39] However, the effect of hydrogen bonding in this TA/PnPropOx system and the role of temperature and pH in film and capsule properties such as morphology, thickness, permeability, swelling, and shrinking of capsules are yet unexplored. In this paper, we demonstrate the fabrication of TA/PnPropOx multilayer films and capsules and provide a detailed investigation on the role of temperature and pH in film formation, stability, and permeability. The chemical structures of the PnProPOx, TA, and fluorescent molecules used for confocal laser scanning microscopy (CLSM) investigations are shown in Scheme 1. We believe that both hydrogen bonding and hydrophobic interactions can play an important role in enhancing the stability of films and capsules, while electrostatic forces and hydrophobic interactions are involved in deciding the location and degree of filling of capsules. The mechanistic insights obtained from the current study will be useful to develop a controlled drug delivery system based on TA/PnPropOx and design the release profile for in vivo applications in future work.

2. EXPERIMENTAL SECTION

2.1. Materials. TA, poly(sodium 4-styrene sulfonate) (MW = 70 kDa), FITC-dextran (MW = 70 kDa), TRITC-dextran (MW = 65−85 kDa), rhodamine, 6-carboxyfluorescein, $CaCl_2$, Na_2CO_3, and ethylenediaminetetraacetic acid (EDTA) were purchased from Sigma-Aldrich, India, and used without any further purification. PnPropOx with a degree of polymerization (DP) of 100 was synthesized by cationic ring-opening polymerization as previously reported.[40] Size exclusion chromatography with *N*,*N*-dimethyl acetamide containing LiCl as an eluent was used for characterization of synthesized polymers, and the obtained results are summarized in Table S1 (Supporting Information). Milli-Q water with a resistivity greater than 18 MΩ cm was used for confocal microscopy investigations and fabrication of multilayer thin films and capsules.

2.2. Preparation of Substrates for LbL Assembly. Quartz substrates of dimension 1 cm × 5 cm were used for UV−visible (UV−vis) measurements to investigate the film growth. Prior to LbL assembly, the quartz substrates were cleaned with a piranha solution for 10 min under ultrasound treatment before use. **Caution!** Piranha is highly corrosive and should be handled with extreme care and should not be stored in closed containers. The substrates were washed three times with water, dried in a nitrogen stream, and used for LbL assembly. The same cleaning procedure was used to prepare silicon wafer substrates (8 mm × 8 mm) to obtain information about morphological changes and thickness of the LbL-assembled films using scanning electron microscopy (SEM), atomic force microscopy (AFM), and profilometry.

2.3. Fabrication of Hydrogen-Bonded TA/PnPropOx Thin Films. PnPropOx (1 mg mL^{-1}) and TA (1 mg mL^{-1}) solutions were made with Milli-Q water and stored overnight in a refrigerator at 4 °C. The multilayer thin films were assembled on quartz substrates by successively dipping the substrates in the TA and PnPropOx solutions. First, a TA layer was fabricated on quartz substrates by immersing the substrates in TA solution for 10 min as it interacts strongly with the surface. After adsorption, the TA-coated substrates were rinsed three times with Milli-Q water for 1 min to remove loosely bound TA molecules from the surface. The substrates were then dried with a stream of nitrogen for 1 min and kept in PnPropOx solution to continue the LbL assembly process. Deposition of one TA layer and one PnPropOx layer is regarded as one LbL cycle and is termed a single bilayer formation. This process of sequential adsorption and rinsing was repeated to obtain the desired number of TA/PnPropOx bilayers. After each bilayer formation, UV−vis spectra were acquired to investigate the film growth. The assembly was performed at 15 °C in an Incufridge (RS-IF-203, Revolutionary Science) or by varying the temperature in a temperature-controlled incubator shaker to investigate the influence of temperature on the LbL assembly process. To investigate the influence of assembly pH on film formation, the pH of the polymer solutions and rinsing water was adjusted with 0.1 M NaOH or HCl before use. Control films for investigating the influence of pH or temperature on film formation were assembled using freshly prepared solutions of TA (pH 4.5) and PnPropOx (pH 6) solutions at 15 °C and pH ≈ 6. For morphological characterization, the assembled films were dried with a nitrogen stream and stored in a closed container before characterization.

2.4. Calcium Carbonate Microparticle Preparation. Coprecipitation method was used to prepare calcium carbonate microparticles, wherein equimolar solutions (0.3 M) of $CaCl_2$ and Na_2CO_3 were mixed under continuous stirring.[6,41] The mixture turned into turbid suspension instantaneously that confirmed the formation of $CaCO_3$ microparticles. After completion of the reaction, $CaCO_3$ microparticles were filtered and washed five times with water in a membrane filtration setup using a cellulose filter paper having a pore size of 0.45 μm. The filtered $CaCO_3$ microparticles were air-dried overnight and used as sacrificial templates for hollow capsule preparation. $CaCO_3$ microparticles doped with poly(sodium styrene sulfonate) (PSS-$CaCO_3$) were also prepared by dissolving PSS (final concentration, 2 mg mL^{-1}) in Na_2CO_3 solution before mixing with $CaCl_2$ solution.

2.5. TA/PnPropOx Capsule Preparation. The synthesized $CaCO_3$ (control and PSS-doped) microparticles were used as sacrificial templates for TA/PnPropOx capsule fabrication. The temperature of the polymer solutions and washing water was maintained at 15 °C, and LbL assembly was performed in an Incufridge at 15 °C. For capsule fabrication, the microparticles (7.5 mg mL^{-1}) were dispersed in 2 mL of water under ultrasonic treatment for 1 min in 2 mL of centrifuge tubes and washed three times with Milli-Q water in a low-temperature centrifuge at 8000 rpm (Hermle Z216 MK, Germany). The washed $CaCO_3$ particles were first dispersed in 2 mL of TA solution (1 mg mL^{-1}) to start the assembly process and allowed for deposition for 15 min. After separating the coated particles by centrifugation process at 8000 rpm, the particles were washed three times with water to remove free TA in the supernatant. The TA-coated $CaCO_3$ particles were dispersed again in PnPropOx solution (1 mg mL^{-1}), and these deposition and washing steps were continued for TA and PnPropOx. After the deposition of two bilayers, the coated $CaCO_3$ particles were dispersed in 0.2 M EDTA solution for 30 min (three times) and washed five times with water to obtain hollow capsules. The prepared hollow capsules were stored in a closed container at 4 °C and used for further experiments.

To investigate the swelling of the capsules as a function of pH, the pH of the control (with or without PSS) capsules varied from pH 2 to 9.5 and imaged using SEM and CLSM. Control capsules were also treated at different temperatures to investigate the influence of temperature on the morphology of capsules. Control capsules for investigating the influence of pH or temperature on capsule surface

DOI: 10.1021/acs.langmuir.9b02938
Langmuir 2019, 35, 14712−14724

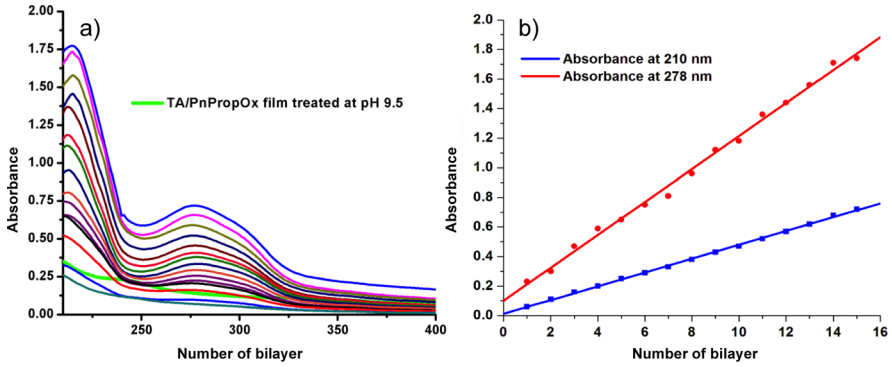

Figure 1. UV−vis spectra obtained for the LbL assembly of PnPropOx and TA showing the growth of multilayer films as a function of the number of bilayers. (a) UV−vis spectra and (b) absorbance values at 210 and 278 nm as a function of number of bilayers. Freshly prepared polymer solutions in Milli-Q water were used for LbL assembly without adjusting the pH (assembly pH of ∼6).

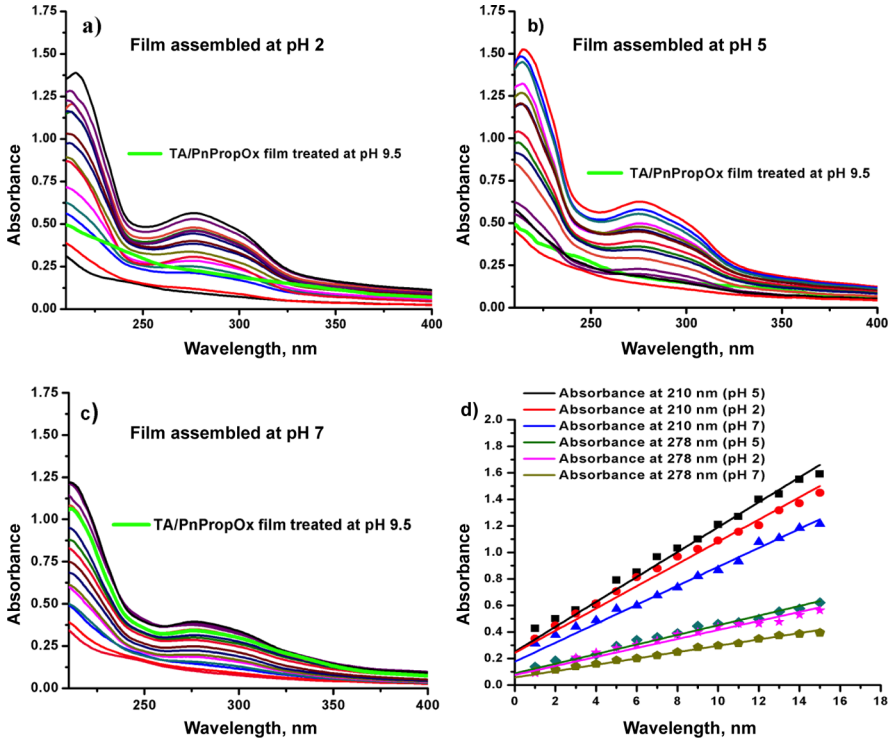

Figure 2. UV−vis spectra showing the growth of the multilayer films as a function of the number of bilayers prepared at different pH values. Films assembled at (a) pH 2, (b) pH 5, and (c) pH 7 and their absorbance values at 210 and 278 nm (d). Spectra appeared in green color in images (a−c) indicate the dissolution/stability of the films after treating the assembled films at pH 9.5.

morphology were assembled using freshly prepared solutions of TA and PnPropOx at 15 °C and pH ≈ 6.

2.6. UV−Vis Spectroscopy. UV−vis spectroscopy was used to investigate the thin-film growth on quartz substrates by measuring the increase of absorbance as a function of layer number (Nanodrop 2000c Spectrophotometer, Nanodrop Technologies, USA). After the deposition of each bilayer, the absorption spectrum was recorded in transmission mode by placing the film-deposited substrates across the laser beam in a cuvette.

2.7. Confocal Laser Scanning Microscopy. Hollow capsules were visualized by mixing a fluorescent probe solution (0.2 mg mL^{-1}) to the capsule suspension using an LSM 600 confocal scanning system (Zeiss, Germany) equipped with a 100×/1.4−1.7 oil immersion objective. Fluorescent molecules of varying hydrodynamic diameters and charges were used as model molecules to study the shell permeability and stability of the capsules. To investigate the capsule stability at different pH values, the capsules were incubated in different pH values of water for 3 h and added with fluorescent molecules prior to CLSM imaging. CLSM imaging was performed by placing 10 μL of the capsule suspension on a microscopic slide and images were acquired at 40× or 63× magnification. Imaging parameter such as aperture, gain, and laser power were kept constant for all the experiments to avoid oversaturation of the fluorescence signal during imaging. The lasers with an excitation wavelength of 488 nm for FITC-dextran and carboxyfluorescein and 540 nm for rhodamine and TRITC-dextran were used for CLSM imaging.

2.8. Atomic Force Microscopy. Morphological changes of capsules and films were investigated using AFM (NTEGRA Prima-NTMDT AFM, Spectrum Instruments Ltd., Ireland) in tapping mode. For preparation of AFM samples, dilute capsule suspension was placed on cleaned silicon wafers and air-dried overnight in a desiccator to remove the moisture completely.

2.9. Profilometery. Thickness and roughness of the multilayer thin films were measured by Stylus Profilometer (DektakXT, Bruker, Germany) in a dry state. The thickness values of multilayer thin films were measured by forming a scratch on the film with a sharp razor

DOI: 10.1021/acs.langmuir.9b02938
Langmuir 2019, 35, 14712−14724

blade. The thickness values were estimated by drawing a line profile across the scratch.

2.10. Scanning Electron Microscopy. Morphological investigations of multilayer thin films were performed using SEM by sputtering a thin gold layer (≈5 nm) on air-dried multilayer thin films deposited on silicon substrates. For SEM imaging of hollow capsules, a drop of capsule suspension was placed on a silicon wafer, air-dried overnight, sputter-coated with a thin layer of gold, and imaged under a field emission scanning electron microscope at an operating voltage of 5 kV (FESEM-SUPRA 55, Carl Zeiss, Germany).

3. RESULTS AND DISCUSSION

PnPropOx with a DP of 100 and a relatively narrow molar mass distribution, that is, a dispersity ($Đ$) of 1.23, was synthesized by living cationic ring-opening polymerization of 2-*n*-propyl-2-oxazoline (Table S1, Supporting Information).[40] This rather low molar mass polymer was chosen as it has better aqueous solubility in water below 23 °C and undergoes configurational reorganization at physiological temperature, that is, lower critical solution temperature (LCST). As the entropy of mixing is unfavorable at $T > 23$ °C, the polymer becomes hydrophobic and insoluble in water upon heating, and hence, the assembled capsules can be used for temperature-responsive drug delivery applications.

3.1. Investigation of TA/PnPropOx Multilayer Thin Films. The LbL assembly of PnPropOx and TA on a quartz substrate was investigated by UV−vis spectroscopy by measuring the increase in absorbance as a function of the number of layers (Figure 1). The UV−vis spectra show two characteristic peaks at 278 and 210 nm, which are corresponding to a combined peak resulting from the $\pi \rightarrow \pi^*$ transition of TA and the amide groups of PnPropOx and the phenyl groups of TA, respectively.[42] Notably, the growth as a function of the number of layers is linear at pH 6, that is, the amount of the adsorbed polymer is constant for each bilayer deposition. The layer growth is driven by the hydrogen bonding between the amide groups of PnPropOx as hydrogen bond acceptors and the multiple phenol groups of TA as hydrogen bond donors in combination with hydrogen bonding-induced dehydration.[19] Interestingly, post-treatment of the assembled films with water at pH 9.5 for 2 h showed the disappearance of both the characteristic peaks in the UV−vis spectrum, which indicated the dissolution of the films. It is speculated that deprotonation of TA at higher pH values leads to a decrease in the interactions between the different layers of PnPropOx and TA eventually leading to destabilization and dissolution of the films.

To further understand the influence of pH on the LbL assembly of TA and PnPropOx, the film formation was carried out at different pH values varying from 2 to 9. Prior to LbL assembly, the pH of the polymer solution, TA, and Milli-Q water (for rinsing) was adjusted to assembly pH with 0.1 M HCl or NaOH. After each bilayer deposition at the different pH values, a UV−vis spectrum was acquired to investigate the layer growth. These UV−vis investigations showed that film formation was observed up to pH 7 (Figure 2) while no deposition occurred at pH 9. This observation can be ascribed to the deprotonation of TA at higher pH values interfering with its hydrogen bonding ability and increasing its aqueous solubility. At pH 2, 5, and 7, two characteristic peaks at 278 and 210 nm were observed after LbL assembly and the absorbance increased linearly as a function of the number of bilayers at these pH values, demonstrating that the LbL build-up follows a linear growth regime and that the film build-up is constant and uniform. The absorbance of the $(TA/PnPropOx)_{15}$ film at 210 nm is 1.52 when assembled at pH 5, while it is 1.38 and 1.21 at pH 2 and 7, respectively (Supporting Information, Table S2). This decrease in absorbance values at pH 2 and 7 indicates a decrease of the amount of adsorbed material assuming that the extinction coefficients do not vary at the different pH values, which seems justified by the observation that the UV−vis spectra for assembly at different pH values show very similar features. Furthermore, the film thickness was determined by AFM, revealing that the film thickness for 15 bilayers of TA/PnPropOx (control film assembled at pH ≈ 6) was found to be 160 ± 20 nm. When the assembly pH was increased from 2 to 7, the film thickness increased from 125 ± 20 nm at pH 2 to 145 ± 20 at pH 5 and then started to decrease to 88 ± 20 nm at pH 7 (Supporting Information, Figures S1−S3). These observed film thicknesses are in accordance with the decrease of UV−vis absorption observed for films assembled at higher or lower pH values, indicating the adsorption of smaller amounts of polymer and TA. A previous report on PIPOX demonstrated that enhanced hydrophobic interactions among isopropyl groups at pH > 5 lead to decreased solubility and formation of aggregates.[43] At acidic pH ranges (pH < 5), PIPOX exists as isolated chains or as a cluster of only few molecules with a size of about 4 nm, which transforms into larger aggregates (hydrodynamic diameter = ∼370 nm) at higher pH values. On the basis of this report, it is proposed that the fastest LbL growth rate at pH 5 results from the deposition of hydrophobic PnPropOx clusters with protonated TA that can also interact with itself, further enhancing the film growth. At pH 2, PnPropOx will interact more strongly with H_3O^+, leading to less PnPropOx deposition, while at pH 7, TA will be partially deprotonated, leading to less TA deposition. To investigate the stability of the obtained $(TA/PnPropOx)_{15}$ films at pH > 9, the assembled films were incubated in water of pH 9.5 and the absorbance was investigated using UV−vis. Similar to the films that were assembled without adjusting the solution pH (Figure 1), the disappearance of characteristic peaks was observed for the films assembled at pH 2 and 5. Unexpectedly, it was observed that the film assembled at pH 7 was quite stable at pH 9.5 as only a minor drop in UV−vis absorbance occurred after incubation for 2 h at pH 9.5. This indicates that the films assembled at pH 7 are more stable than that of other films. A similar observation was reported by Demirel and co-workers for poly(*N*-vinylpyrrolidone)-TA LbL films that were pH-annealed at pH 7.[44] The enhanced stability of the films was attributed to relaxation of kinetically trapped molecules in the films, which may also be the case in our capsules.

To gain more detailed information about the role of pH in film stability, the control $(TA/PnPropOx)_{15}$ films prepared in Milli-Q water were treated at different pH conditions and investigated by UV−vis spectroscopy and SEM. The UV−vis spectra of the films showed clear peaks at 278 and 210 nm when treated with a solution having pH up to 9, which disappeared upon treatment at pH 9.5, indicating the dissolution of the film (Figure 3). Notably, SEM investigations showed that the initial sample was smooth, indicating the uniform deposition of multilayer films, as shown in Figure 4a. It is worth noting that the drying process resulted in the formation of cracks on the surface of the films. When these films were treated at different pH values, there were no significant morphological changes in the pH range between 2

DOI: 10.1021/acs.langmuir.9b02938
Langmuir 2019, 35, 14712−14724

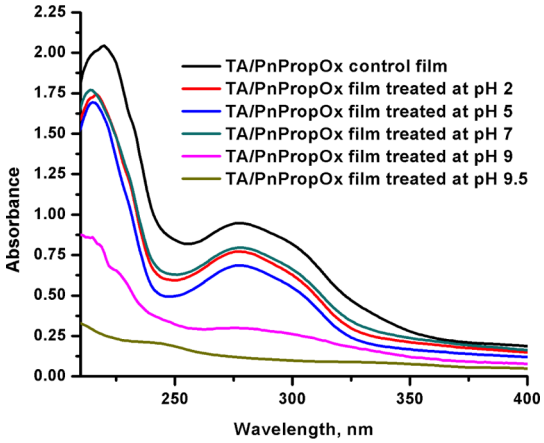

Figure 3. UV−vis spectra of control $(TA/PnPropOx)_{15}$ films and films treated at different pH values for 2 h. Control films were prepared with freshly prepared polymer and TA solutions in Milli-Q water at pH ≈ 6.

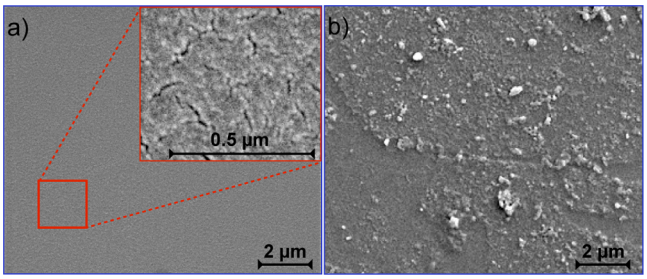

Figure 4. SEM image shows the morphology of (a) control $(TA/PnPropOx)_{15}$ multilayer films (assembled at 15 °C and pH ≈ 6) and (b) same film treated at pH 9 for 2 h. Inset shows the red marked area at higher magnification.

and 7 (Supporting Information, Figure S4). Interestingly, the morphology of the films drastically changed from a smooth pore-free film to a porous film with significant discontinuities (Figure 4b) at pH 9. It demonstrated that films were stable in the pH window between 2 and 9 as shown in Figure 3 and Supporting Information, Figure S4. It is worth noting that the decrease in the absorbance of the film at pH 9 indicates significant loss of the film. As these films revealed cracks and discontinuities, thickness measurements could not be performed with AFM measurements, which resulted in non-consistent thickness and roughness measurements. To avoid errors in thickness and roughness measurements, profilometry was used to measure the thicknesses of the initial and treated films.

Next, the effect of the LbL assembly temperature was investigated in between 5 and 22 °C, which are all below the LCST phase-transition temperature, whereby the lower hydration of the polymer at higher temperatures is anticipated to lead to more efficient PnPropOx deposition. Freshly prepared polymer solutions (pH of TA is 4.5 and pH of PnPropOx is 6) were used to fabricate multilayer thin films for investigation of influence of temperature on film growth. Prior to LbL assembly, the temperature of the polymer solution, TA, and Milli-Q water was adjusted to the assembly temperatures (e.g., 5, 15, 20, and 22 °C). UV−vis investigations showed that stable film formation was achieved only up to 20 °C (Figure 5). The absorbance value of the assembled films was plotted as a function of the number of bilayers to investigate the growth of the films (Figure 5d). The two characteristic peaks at 278 and 210 nm were again observed and the absorbance increased linearly at all temperatures up to 20 °C. Similar to varying pH, the assembly followed a linear growth regime and the film formation was uniform. Interestingly, the film thickness was increased as a function of temperature. For instance, the absorbance of the obtained $(TA/PnPropOx)_{15}$ film at 210 nm is 1.38 at 5 °C, which increases to 1.77 and 2.09 when prepared at 15 and 20 °C, respectively (Supporting Information, Table S2). Furthermore, the film thickness data obtained by profilometry showed that the film thickness for 15 bilayers increased from 130 ± 20 to 210 ± 30 nm when the assembly temperature was increased from 5 to 20 °C. The thickness and roughness of the $(TA/PnPropOx)_{15}$ films also increased significantly when the assembly temperature was increased from 5 to 20 °C, indicating the formation of thicker and rougher films (Supporting Information, Figure S5). Our previous study demonstrated that the mass of PnPropOx adsorbed in TA/PnPropOx films at 5 °C is lower than that of at 20 °C when other assembly conditions are kept constant.[19] This phenomenon is slightly different from that of conventional hydrogen-bonded systems wherein the total enthalpy for the assembly would decrease with the decrease of temperature, which leads to stronger interactions between donor and acceptor molecules. As the enthalpy change for TA/PnPropOx interactions is positive, it was apparent that the decrease in total enthalpy was overcompensated by entropy gain, resulting from the release of hydrating water molecules.[19,45] Consequently, the LbL assembly at increased temperatures that are closer to the phase-transition temperature will lead to more efficient dehydration of PnPropOx upon assembly and, therefore, a higher entropic driving force.

AFM investigation revealed that the assembled films, irrespective of assembly pH and temperature, transformed from pore-free smooth structures at T °C (5, 15, and 20 °C) to porous structures at 37 °C owing to phase segregation of PnPropOx above an LCST temperature of 23 °C by expelling the water molecules, and thereby, forming globules (Supporting Information, Figure S6). The 15 bilayer (TA/PnPropOx) films that were prepared at 5, 15, and 20 °C showed thickness values of 170 ± 20, 220 ± 20, and 250 ± 30 nm, respectively, after heat treatment at 37 °C, revealing a similar trend as the UV−vis investigations (Supporting Information, Figure S7). Notably, all films assembled at different pH values from 2 to 7 show an increase of roughness when the temperature was changed to 37 °C, indicating the gradual change in polymeric configuration from hydrated chains to collapsed globules (Supporting Information, Figure S8). When the films assembled at different temperatures were treated at different pH values, there was no significant difference in the UV−vis spectra and the characteristic peaks were clearly observed up to pH 7. All the films, except the film assembled at 20 °C, showed the disappearance of the characteristic peaks at pH 9.5, demonstrating the complete dissolution of films (Figure 5). However, the film assembled at 20 °C only showed partial disappearance of characteristic peaks and simultaneous appearance of two new peaks centered at 250 and 335 nm (Figure 6). The higher stability of the film that is assembled at 20 °C may be ascribed to the more efficient dehydration of PnPropOx slowing down its rehydration and dissolution. A detailed investigation on the formation of the new peaks in the UV−vis spectrum showed that increasing the pH > 7 resulted in the appearance of the phenolate form of TA at 335 nm,

DOI: 10.1021/acs.langmuir.9b02938
Langmuir 2019, 35, 14712−14724

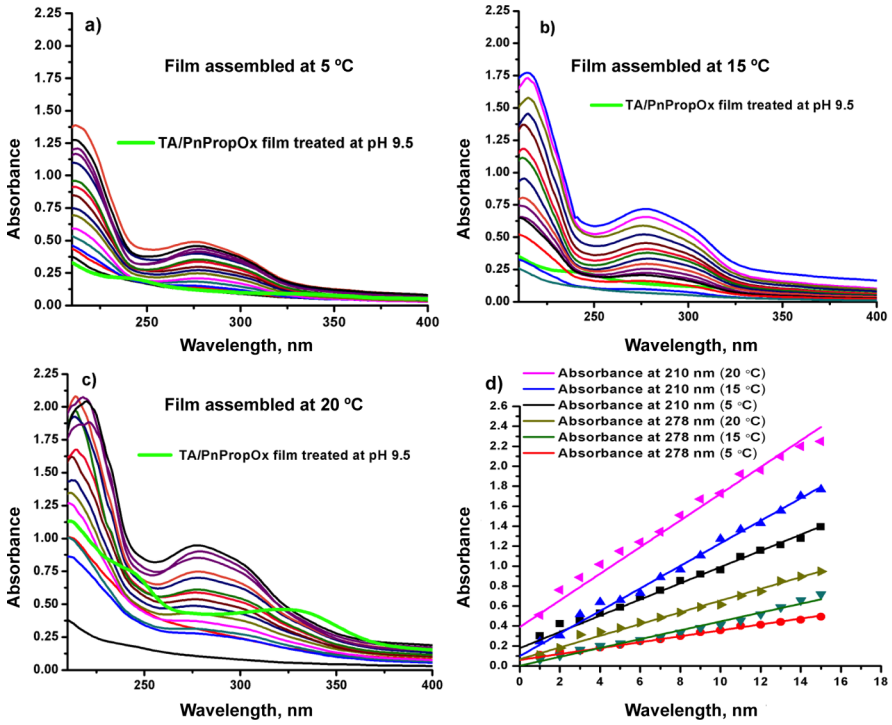

Figure 5. UV−vis investigations show the growth of multilayer films as a function of layer number at different temperatures. Films assembled at (a) 5, (b) 15, and (c) 20 °C and their absorbance values at 210 and 278 nm (d). Spectra appeared in green color (a−c) indicate the dissolution/stability of the films after treating the assembled films at pH 9.5.

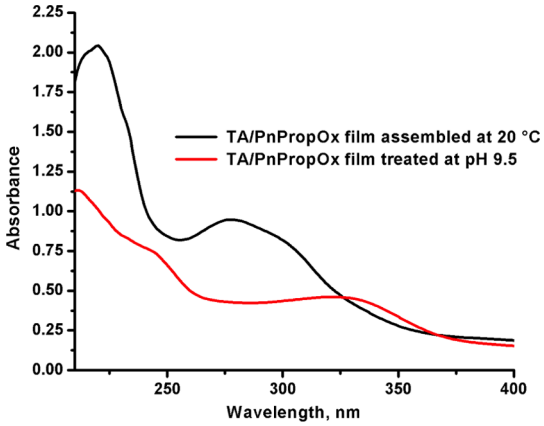

Figure 6. UV−vis investigations show the spectrum of 15 bilayer TA/PnPropOx multilayer film assembled at 20 °C before and after treating the film with pH 9.5 water. For LbL assembly, freshly prepared TA and PnPropOx (without adjusting pH) solutions were maintained at 20 °C.

indicating that increasing the pH induced deprotonation of TA as may be expected. The estimated absorbance ratio A_{335}/A_{279}, an indication of ratio of ionized and neutral forms of TA, was found to be about 48%. Previous reports showed that the pK_{app} value for TA in solution is <3.2,[46] which, however, increased to 7.6 in the form of film for TA/chitosan films,[38] which is in agreement with the observation in this work that the LbL films are stable up to a pH of at least 7.

3.2. Investigation of (TA/PnPropOx)$_2$ Hollow Capsules. Hollow polymeric capsules made of two bilayers of PnPropOx/TA were fabricated using PSS-doped $CaCO_3$ and bare $CaCO_3$ (control) particles as sacrificial templates for LbL assembly. The $CaCO_3$ particles were of spherical shape with a size range of 5−7 μm. A combination of sedimentation and centrifugation processes was used to separate the 5.5 ± 0.5 μm particles after synthesis for LbL assembly. Both pure and PSS-doped $CaCO_3$ particles were used for the LbL assembly, resulting in the formation of a uniform pore-free coating after deposition of two bilayers of TA/PnPropOx (Supporting

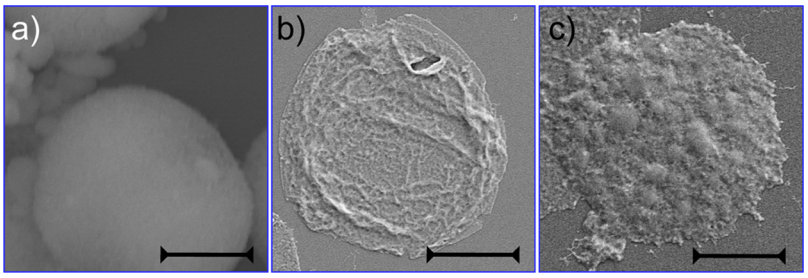

Figure 7. SEM investigations show the morphology of PSS-doped $CaCO_3$ microparticles (a), control hollow capsules obtained from PSS-doped $CaCO_3$ microparticles (b), and bare $CaCO_3$ microparticles (c). Control capsules (with and without PSS) were prepared by depositing freshly prepared TA and PnPropOx solutions on sacrificial bare $CaCO_3$ and PSS-doped $CaCO_3$ microparticles. Scale bar = 2 μm.

DOI: 10.1021/acs.langmuir.9b02938
Langmuir 2019, 35, 14712−14724

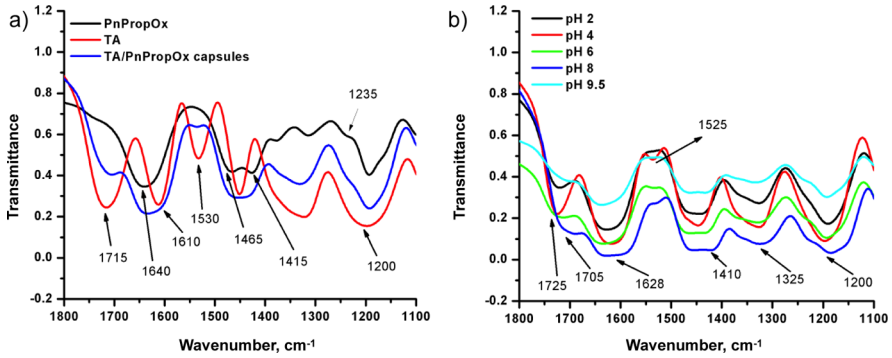

Figure 8. FTIR investigations show the spectra of as-prepared capsules (a) and capsules treated at different pH values (b).

Information, Figure S9) and in the formation of hollow capsules after dissolution of the $CaCO_3$ core with 0.2 M EDTA solution and extensive rinsing with Milli-Q water. The obtained hollow capsules exhibited a collapsed shell with folds and creases that are typical for hollow structure of ultrathin shells.[47,48] Notably, the capsules obtained from bare $CaCO_3$ and PSS-$CaCO_3$ particles are morphologically different owing to the presence of PSS in the interior of the capsules, as shown in Figure 7. Previous reports on PSS-doped $CaCO_3$ particles for poly(allylamine) hydrochloride (PAH)/PSS capsule fabrication showed that a fraction of preloaded PSS molecules get released inside the capsules after template dissolution, which interacts with layer components and form PAH/PSS complex structure at the interior surface of the hollow capsules.[6] As a result, the shell of the capsules obtained from PSS-doped $CaCO_3$ particles was rigid and maintains its physical stability while the shell of the capsules (obtained from bare $CaCO_3$ particles) was soft and freely fills in the inner structure.

Given the stable formation of films at different pH values and temperatures, as investigated by UV−vis and SEM, and with a desire to further elucidate the binding mechanism between TA and PnPropOx, the capsules were investigated by Fourier transform infrared (FTIR) spectroscopy. As shown in Figure 8a and the Supporting Information (Figure S10), two broad absorption bands were present in the range of 3600−3000 cm^{-1} that are characteristic for O−H stretchings of phenolic hydroxyl groups. TA has four sharp characteristic bands at 1715, 1530, 1610, and 1200 cm^{-1}, which are ascribed to C═O stretching, carboxylate ($-COO^-$) asymmetric stretching, C═C vibrations, and the bending vibration of C−O associated with phenolic hydroxyl groups in TA. The PnPropOx spectrum shows characteristic peaks at 2970, 1640, 1465, 1415, and 1235 cm^{-1}, which are corresponding to CH_2 stretching, C═O stretching, C−H deformation, CH_3 symmetrical deformation or CH_2 bending, and C−N stretching, respectively. As the interaction between TA and PnPropOx is mainly attributed to hydrogen bonding, no major differences are expected in the film spectrum, and, indeed, the characteristic peaks of both TA and PnPropOx appear in the spectrum of the capsules, although shifted from their original wavenumber. After capsule formation, the characteristic vibration of the phenol groups (νC−O) in TA remains at 1200 cm^{-1}, while the characteristic band of the aromatic system of TA at 1715 cm^{-1} (νC═O) is lowered to 1705 cm^{-1}, indicating that C═O is engaged in a hydrogen-bonding interaction. The carboxylate ($-COO^-$) asymmetric stretching band intensity at 1530 is reduced and appeared like a shoulder peak that indicated engagement of $-COO^-$ groups in complexation with PnPropOx. Notably, the band appearing in the range of 3100−3500 cm^{-1} becomes broader, indicative of newly formed hydrogen bonds between the phenol groups of TA and amide groups of the PnPropOx polymer chains. After forming a complex with TA, the absorption band of C═O in PnPropOx is lowered to 1628 cm^{-1}, which is also a clear indication of hydrogen bonding.[49] When the capsules were treated at different pH values (Figure 8b), two new peaks appeared at pH > 2 with absorption bands at 1525 and 1410 cm^{-1} that correspond to antisymmetric and symmetric COO^- vibrations. The formed antisymmetric and symmetric COO^- vibrations at pH values between 4 and 8 are sharper and slightly red shifted from their original position, which is a clear indication of the ionization of films at higher pH values.

To get more detailed information about the morphological changes of the capsules, the capsules were treated at different pH values and temperatures and investigated in SEM and AFM (Figures 9 and 10). The as-prepared capsules have a pore-free collapsed structure of a thin polymer shell after template dissolution (Figure 7). Notably, the SEM images of capsules treated with water of different pH values showed that the

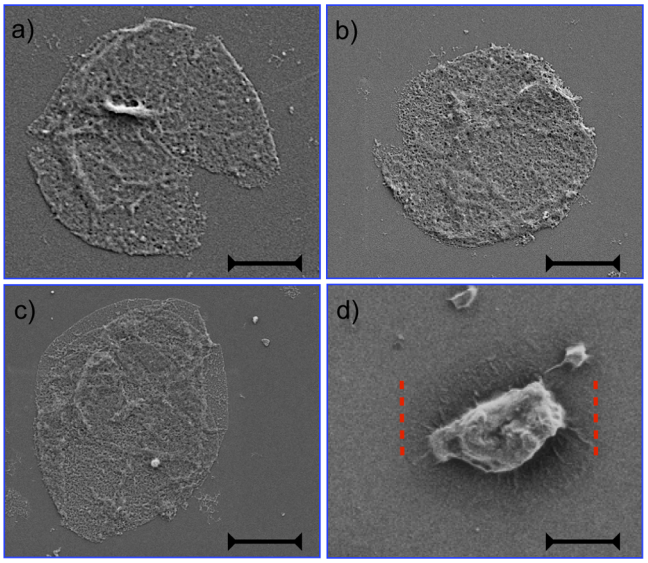

Figure 9. SEM investigations show the morphology of PSS-doped $CaCO_3$ microcapsules at (a) pH 2, (b) pH 3, (c) pH 5, and (d) pH 9.5. The pH of control capsule suspension was adjusted with 0.1 M NaOH or HCl and incubated for 3 h before imaging in SEM. Scale bar = 2 μm.

DOI: 10.1021/acs.langmuir.9b02938
Langmuir 2019, 35, 14712−14724

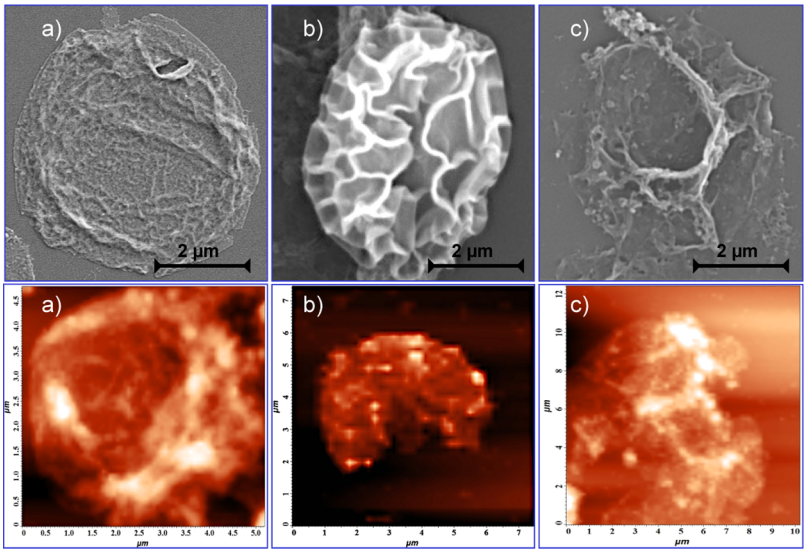

Figure 10. SEM (top panel) and AFM (bottom panel) investigations show the morphology of PSS-doped $CaCO_3$ microcapsules after heat treatment at different temperatures for 2 h. Control capsules assembled at 15 °C (a) and the same capsules treated at 30 (b) and 40 °C (c). The control capsules obtained by depositing freshly prepared PnPropOx and TA solutions on PSS-doped $CaCO_3$ microparticles at 15 °C were used as control capsules.

capsules were stable and intact in the pH range between 2 and 9 as shown in Figure 9. However, the capsules showed breakage and deformed structures at extremely high and lower pH ranges, indicating significant morphological change of the capsules (Figure 9). This is in accordance with the sharper antisymmetric and symmetric COO^- vibrations observed at these pH values in the FTIR spectra, indicating the ionization of TA in the polymeric shell. Interestingly, at pH 9.5, the capsules did not completely dissolve, but instead, the polymeric shell started to shrink from the outer circumference, accumulated, and formed a kind of particle morphology in the center, as shown in Figure 9d. The influence of temperature on capsule morphology was also investigated by incubating the capsule suspensions at various temperatures (Figure 10). At elevated temperatures, the capsules underwent a morphological transformation by forming peaks and valleys on its surfaces and the intact shell was lost after 2 h of heat treatment at 40 °C. It is worth noting that the transformation is faster at 40 °C than at 30 °C.

3.2.1. pH-Dependent Stability of TA/PnPropOx Capsules. The capsules made of two bilayers of TA/PnPropOx that were prepared with 5.5 ± 0.5 μm PSS-$CaCO_3$ templates were used to study the pH-dependent stability using CLSM. The pH of the capsule suspension was varied at least 3 h prior to CLSM investigations and stored at 15 °C to measure the diameter of capsules in equilibrium. FITC-dextran and TRITC-dextran were used as fluorescent probes of varying size for CLSM investigations. The resulting capsule diameter was plotted as a function of pH of the suspension in Figure 11. The diameter of the capsules was almost constant (5.5 ± 0.5 μm) in the intermediate pH range of 3−8.5, confirming that capsules are stable in the intermediate pH range and the hydrogen bonding between the amide groups of PnPropOx and phenol groups of TA is not disrupted by the protonation of the benzoic acid groups, nor by the partial deprotonation of the phenol groups (Figure 11). When the pH was increased above 8.5, shrinking of the capsules was observed and the capsule diameter decreased to 3.75 ± 0.5 μm at pH 9.5, that is, about 32%. Other reported hydrogen-bonded LbL capsules, which start

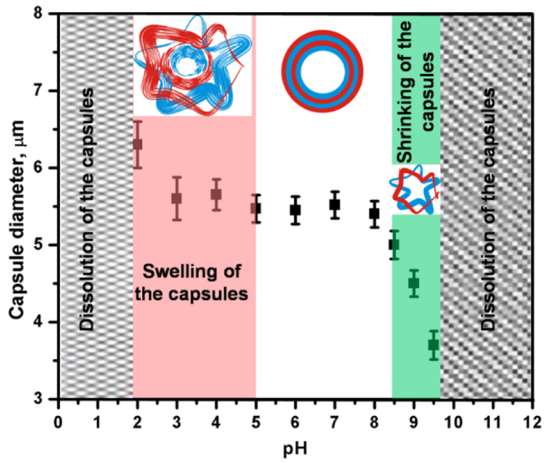

Figure 11. Investigations of capsule diameter as a function of pH.

shrinking at pH ≈ 8, maintain the spherical shape before collapsing at pH > 8.[47,48] In the lower pH range at pH < 3, the capsules start swelling by 20% and reach about 6.6 ± 0.5 μm in size and fully dissolve at pH < 2. As can be seen from FTIR investigations (Figure 8), the intensity bands of the carboxylic groups (at 1525 and 1410 cm^{-1}) decrease at lower pH values. A recent report on PIPOX revealed that the zeta potential increased from ∼0 to +15 mV when pH was decreased from 5.2 to 2.5, that is, pK_a value of PIPOX ∼5.2.[43] Notably, PIPOX existed as larger aggregates at pH > 6 transformed into isolated chains or cluster of few chains, ascribed to protonation of amide groups at lower pH ranges (between pH 2.5 and 5.2), which may also be due to coordination of H_3O^+ to the amide groups.

To get more detailed information about the permeability of the shell at different pH values, the capsules were incubated in water at different pH values and investigated in CLSM in the presence of FITC-dextran, TRITC-dextran, rhodamine, and carboxyfluorescein as model fluorescent molecules at 15 °C (Figure 12). The presence of fluorescence in the interior of the

DOI: 10.1021/acs.langmuir.9b02938
Langmuir 2019, 35, 14712−14724

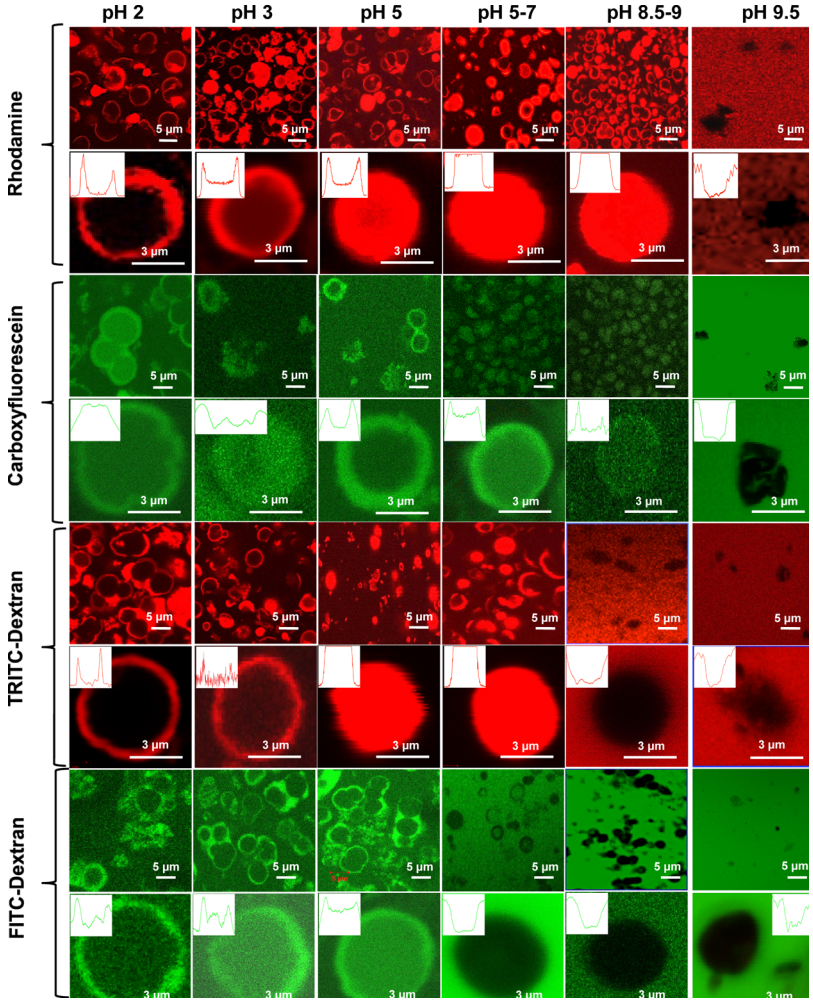

Figure 12. CLSM investigations show the permeability of control capsules (PSS loaded) for different fluorescent molecules as a function of pH. Carboxyfluorescein or FITC-dextran (green color), and rhodamine or TRITC-dextran (red color). Insets show the fluorescence intensity profiles of the individual capsules.

capsules was interpreted as an indication for the capsule permeability against particular fluorescent molecule. For instance, darker (black) capsules are indicative for the impermeable nature of the capsules against a particular fluorescent molecule. To confirm the preferential distribution of the fluorescent molecules either in the shell or in the interior, the fluorescent intensity profiles were drawn across the capsule diameter. The successful and stable encapsulation of fluorescent molecules was confirmed by visualizing the fluorescence in the interior of the capsules after washing with water. When encapsulation was observed for >60% of the capsule population, after washing with water, it was assumed that the capsules were permeable and encapsulation was stable for the fluorescent molecules at that particular pH. Capsules with a fluorescent interior were chosen for drawing intensity profiles. If less than 40% of the capsules had a fluorescent interior, they were considered as either impermeable or empty and we provide intensity profiles for empty capsules. It is worth noting that all images shown in Figure 12 were acquired without washing the capsule suspension. Schematic illustration to indicate the permeability of different fluorescent molecules is shown in Figure 13. In the acidic pH range between 2 and 5, the capsules are permeable to all four fluorescent molecules. Notably, the capsules appear aggregated with an uneven shell

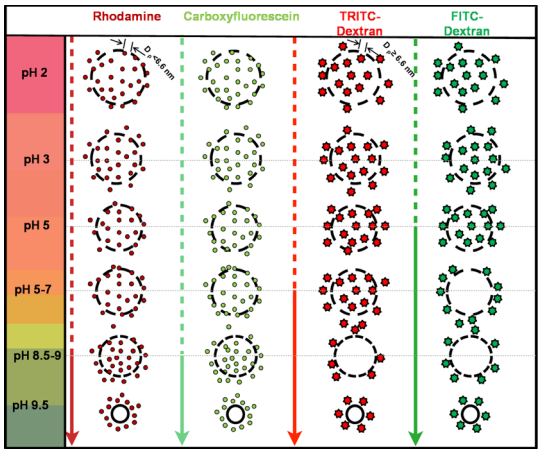

Figure 13. Schematic illustration showing the permeability of $(TA/PnProPOx)_2$ capsules as a function of pH for different fluorescent molecules. The capsules obtained from PSS-$CaCO_3$ microparticles were incubated in pH-adjusted water for 3 h.

thickness (Supporting Information, Figures S11 and S12), most likely induced by morphological transformation of PnPropOx as well as protonation of TA, and potential interaction with H_3O^+.[43] Although the suspension showed a

DOI: 10.1021/acs.langmuir.9b02938
Langmuir 2019, 35, 14712−14724

mixture of empty and filled capsules in this pH range, washing of the capsule suspension with water showed the absence of fluorescence molecules in the interior of the capsules, indicating the presence of larger pores in the shell allowing to washout the fluorescent dye (Supporting Information, Figure S13). As reported in our previous study, the presence of nanopores of size >6 nm on the capsule surface caused the free movement of all fluorescent molecules across the capsule shell.[7] When the pH of the capsule suspension further reduced, the capsules are no longer stable and break into small pieces (Supporting Information, Figure S14). Notably at pH 7, the capsules were permeable to all three fluorescent molecules except FITC-dextran. This indicated that the presence of nanopores of size ≤6 nm on the capsule surface, potentially in combination with repulsion from PSS molecules and/or partially deprotonated TA, prevents the entry of FITC-dextran into the capsules.[7,41] As carboxyfluorescein is a small molecule (hydrodynamic diameter of ∼0.9 nm), it is able to move freely across the polymer shell. After washing the capsule suspension with Milli-Q water, it was observed that only positively charged fluorescent probes (rhodamine and TRITC-dextran) were successfully loaded in the interior of the capsules while negatively charged probes such as carboxyfluorescein and FITC-dextran were limited only to the capsule shell (Supporting Information, Figure S15). The difference in permeability between carboxyfluorescein and FITC-dextran at pH 7 indicated that configurational changes of shell not only resulted in decrease in the average size of pores on the shell but also involve in generation of net negative potential in the capsules owing to deprotonation of TA. At higher pH range (from pH 8.5 to 9), the capsules are permeable only to carboxyfluorescein and rhodamine, indicating the closure of surface pores on the shell (Figure 12 and Supporting Information, Figure S16). Shrinking of the capsules is observed at pH 9 followed by dissolution at pH 9.5. At pH 9.5, the capsules are not stable and appear as polymeric particles of random shape and size. In this pH range, the capsules are not permeable for any molecules, which indicate that the capsules have shrunken to an extent wherein surface pores are small enough to prevent the entry of even small fluorescent molecules such as rhodamine and carboxyfluorescein. Of note, we have also performed similar experiments with PSS-free $(TA/PnProPOx)_2$ capsules and the permeability is similar as explained above, indicating that the net potential as well as the average size of pores present in the shell plays an important role in permeability and encapsulation of $(TA/PnProPOx)_2$ capsules (Supporting Information, Figures S17−S20). The high intensity fluorescence in the interior of the capsules at lower pH conditions also indicate a stronger interaction between dextran molecules and the capsules, most likely hydrogen bonding between the sugar units of dextran and amide units of PnPropOx. At higher pH values, the deprotonated TA units carrying the negative potential along with reduction in the pore size of the shell play an important role in restricting the permeability of the dextran molecules. We believe that the driving force for the encapsulation of positively charged fluorescent molecules in PSS-free $(TA/PnProPOx)_2$ capsules is the electrostatic interaction between the TRITC groups of dextran and deprotonated TA units.

4. CONCLUSIONS

A detailed investigation of hydrogen-bonded TA/PnPropOx multilayer thin films and capsules assembled via LbL assembly is reported. The physicochemical properties of films such as film growth, morphology, and stability are largely dependent on assembly pH and temperature. Films can be assembled up to a pH of 7 or a temperature of 20 °C, and the layer build-up follows a linear growth mechanism at all pH (2−7) and temperature ranges (5−20 °C). Interestingly, TA/PnPropOx multilayer thin films and capsules show better stability over a wide pH range of 2−9, compared to other hydrogen-bonded capsule systems, which may be related to the dehydration of the PnPropOx during LbL assembly. A detailed investigation into the stability of the capsules revealed that capsules shrink and transform into randomly shaped particles at pH 9.5 while capsules undergo swelling process, followed by breakage of capsules at pH < 2. Permeability investigations show that capsules are permeable for all fluorescent molecules at pH ≤ 5 (e.g., FITC-dextran, rhodamine, carboxyfluorescein, and TRITC-dextran), whereas capsules are fully impermeable at pH > 9. Both the surface potential and the average pore size of the shell could influence the permeability and encapsulation of TA/PnPropOx capsules. In future experiments, the role of side chains at 2-position in poly(2-oxazoline) in permeability and encapsulation of capsule systems will be investigated in detail as the side chains govern the balance between the hydrophilic and hydrophobic forces in the capsules.

■ ASSOCIATED CONTENT

Supporting Information

The Supporting Information is available free of charge on the ACS Publications website at DOI: 10.1021/acs.langmuir.9b02938.

Morphological information of TA/PnPropOx multilayer thin films and CLSM investigations of TA/PnPropOx capsules (PDF)

■ AUTHOR INFORMATION

Corresponding Authors

*E-mail: richard.hoogenboom@ugent.be (R.H.).
*E-mail: rsanandhakumar@gmail.com (A.S.).

ORCID

Richard Hoogenboom: 0000-0001-7398-2058
Anandhakumar Sundaramurthy: 0000-0001-6870-7318

Notes

The authors declare no competing financial interest.

■ ACKNOWLEDGMENTS

A.S. acknowledges the financial support from the Department of Science and Technology (DST)—Science and Engineering Research Board (SERB), Government of India (YSS/2015/000771). R.H. and M.V. acknowledge Ghent University and the FWO Flanders for funding.

■ REFERENCES

(1) De Geest, B. G.; Vandenbroucke, R. E.; Guenther, A. M.; Sukhorukov, G. B.; Hennink, W. E.; Sanders, N. N.; Demeester, J.; De Smedt, S. C. Intracellularly Degradable Polyelectrolyte Microcapsules. *Adv. Mater.* **2006**, *18*, 1005−1009.

(2) Antipov, A. A.; Sukhorukov, G. B.; Donath, E.; Möhwald, H. Sustained Release Properties of Polyelectrolyte Multilayer Capsules. *J. Phys. Chem. B* **2001**, *105*, 2281−2284.

(3) Sukhishvili, S. A. Responsive Polymer Films and Capsules via Layer-by-Layer Assembly. *Curr. Opin. Colloid Interface Sci.* **2005**, *10*, 37−44.

DOI: 10.1021/acs.langmuir.9b02938
Langmuir 2019, 35, 14712−14724

(4) Angelatos, A. S.; Radt, B.; Caruso, F. Light-Responsive Polyelectrolyte/Gold Nanoparticle Microcapsules. *J. Phys. Chem. B* **2005**, *109*, 3071−3076.
(5) Anandhakumar, S.; Vijayalakshmi, S. P.; Jagadeesh, G.; Raichur, A. M. Silver Nanoparticle Synthesis: Novel Route for Laser Triggering of Polyelectrolyte Capsules. *ACS Appl. Mater. Interfaces* **2011**, *3*, 3419−3424.
(6) Tong, W.; Dong, W.; Gao, C.; Möhwald, H. Charge-Controlled Permeability of Polyelectrolyte Microcapsules. *J. Phys. Chem. B* **2005**, *109*, 13159−13165.
(7) Paramasivam, G.; Vergaelen, M.; Ganesh, M.-R.; Hoogenboom, R.; Sundaramurthy, A. Hydrogen bonded capsules by layer-by-layer assembly of tannic acid and poly(2-n-propyl-2-oxazoline) for encapsulation and release of macromolecules. *J. Mater. Chem. B.* **2017**, *5*, 8967−8974.
(8) Cortez, M. L.; De Matteis, N.; Ceolín, M.; Knoll, W.; Battaglini, F.; Azzaroni, O. Hydrophobic Interactions Leading to a Complex Interplay Between Bioelectrocatalytic Properties and Multilayer Meso-organization in Layer-by-Layer Assemblies. *Phys. Chem. Chem. Phys.* **2014**, *16*, 20844−20855.
(9) Yang, H.; Yuan, B.; Zhang, X.; Scherman, O. A. Supramolecular Chemistry at Interfaces: Host-Guest Interactions for Fabricating Multifunctional Biointerfaces. *Acc. Chem. Res.* **2014**, *47*, 2106−2115.
(10) Lvov, Y.; Antipov, A. A.; Mamedov, A.; Möhwald, H.; Sukhorukov, G. B. Urease Encapsulation in Nanoorganized Microshells. *Nano Lett.* **2001**, *1*, 125−128.
(11) Boudou, T.; Kharkar, P.; Jing, J.; Guillot, R.; Pignot-Paintrand, I.; Auzely-Velty, R.; Picart, C. Polyelectrolyte Multilayer Nanoshells with Hydrophobic Nanodomains for Delivery of Paclitaxel. *J. Controlled Release* **2012**, *159*, 403−412.
(12) Kempe, K.; Ng, S. L.; Gunawan, S. T.; Noi, K. F.; Caruso, F. Intracellularly Degradable Hydrogen-Bonded Polymer Capsules. *Adv. Funct. Mater.* **2014**, *24*, 6187−6194.
(13) Anandhakumar, S.; Sasidharan, M.; Tsao, C.-W.; Raichur, A. M. Tailor-Made Hollow Silver Nanoparticle Cages Assembled with Silver Nanoparticles: An Efficient Catalyst for Epoxidation. *ACS Appl. Mater. Interfaces* **2014**, *6*, 3275−3281.
(14) del Mercato, L. L.; Abbasi, A. Z.; Ochs, M.; Parak, W. J. Multiplexed Sensing of Ions with Barcoded Polyelectrolyte Capsules. *ACS Nano* **2011**, *5*, 9668−9674.
(15) del Mercato, L. L.; Ferraro, M. M.; Baldassarre, F.; Mancarella, S.; Greco, V.; Rinaldi, R.; Leporatti, S. Biological Applications of LbL Multilayer Capsules: From Drug Delivery to Sensing. *Adv. Colloid Interfac. Sci.* **2014**, *207*, 139−154.
(16) Wang, P.; Kankala, R. K.; Fan, J.; Long, R.; Liu, Y.; Wang, S. Poly-L-ornithine/fucoidan-Coated Calcium Carbonate Microparticles by Layer-by-Layer Self-Assembly Technique for Cancer Theranostics. *J. Mater. Sci. Mater. Med.* **2018**, *29*, 68.
(17) Erel, I.; Schlaad, H.; Demirel, A. L. Effect of Structural Isomerism and Polymer end Group on the pH-Stability of Hydrogen-Bonded Multilayers. *J. Colloid Interface Sci.* **2011**, *361*, 477−482.
(18) da Fonseca Antunes, A. B.; Dierendonck, M.; Vancoillie, G.; Remon, J. P.; Hoogenboom, R.; De Geest, B. G. Hydrogen Bonded Polymeric Multilayer Films Assembled Below and Above the Cloud Point Temperature. *Chem. Commun.* **2013**, *49*, 9663−9665.
(19) Sundaramurthy, A.; Vergaelen, M.; Maji, S.; Auzély-Velty, R.; Zhang, Z.; De Geest, B. G.; Hoogenboom, R. Hydrogen Bonded Multilayer Films Based on Poly(2-oxazoline)s and Tannic Acid. *Adv. Healthcare Mater.* **2014**, *3*, 2040−2047.
(20) Yang, S. Y.; Rubner, M. F. Micropatterning of Polymer Thin Films with pH-Sensitive and Cross-Linkable Hydrogen-Bonded Polyelectrolyte Multilayers. *J. Am. Chem. Soc.* **2002**, *124*, 2100−2101.
(21) Yang, S. Y.; Lee, D.; Cohen, R. E.; Rubner, M. F. Bioinert Solution-Cross-Linked Hydrogen-Bonded Multilayers on Colloidal Particles. *Langmuir* **2004**, *20*, 5978−5981.
(22) Anandhakumar, S.; Debapriya, M.; Nagaraja, V.; Raichur, A. M. Polyelectrolyte Microcapsules for Sustained Delivery of Water-Soluble Drugs. *Mater. Sci. Eng. C. Mater. Biol. Appl.* **2011**, *31*, 342−349.
(23) Richert, L.; Boulmedais, F.; Lavalle, P.; Mutterer, J.; Ferreux, E.; Decher, G.; Schaaf, P.; Voegel, J.-C.; Picart, C. Improvement of Stability and Cell Adhesion Properties of Polyelectrolyte Multilayer Films by Chemical Cross-Linking. *Biomacromolecules* **2004**, *5*, 284−294.
(24) Park, S.-Y.; Bok, S.-H.; Jeon, S.-M.; Park, Y. B.; Lee, S.-J.; Jeong, T.-S.; Choi, M.-S. Effect of rutin and tannic acid supplements on cholesterol metabolism in rats. *Nutr. Res.* **2002**, *22*, 283−295.
(25) Chung, K.-T.; Wong, T. Y.; Wei, C.-I.; Huang, Y.-W.; Lin, Y. Tannins and Human Health: A Review. *Crit. Rev. Food Sci. Nutr.* **1998**, *38*, 421−464.
(26) Lorson, T.; Lübtow, M. M.; Wegener, E.; Haider, M. S.; Borova, S.; Nahm, D.; Jordan, R.; Sokolski-Papkov, M.; Kabanov, A. V.; Luxenhofer, R. Poly(2-oxazoline)s based biomaterials: A comprehensive and critical update. *Biomaterials* **2018**, *178*, 204−280.
(27) Moreadith, R. W.; Viegas, T. X.; Bentley, M. D.; Harris, J. M.; Fang, Z.; Yoon, K.; Dizman, B.; Weimer, R.; Rae, B. P.; Li, X.; Rader, C.; Standaert, D.; Olanow, W. Clinical development of a poly(2-oxazoline) (POZ) polymer therapeutic for the treatment of Parkinson's disease - Proof of concept of POZ as a versatile polymer platform for drug development in multiple therapeutic indications. *Eur. Polym. J.* **2017**, *88*, 524−552.
(28) Wyffels, L.; Verbrugghen, T.; Monnery, B. D.; Glassner, M.; Stroobants, S.; Hoogenboom, R.; Staelens, S. μPET Imaging of the Pharmacokinetic Behavior of Medium and High Molar Mass (89)Zr-Labeled Poly (2-Ethyl-2-Oxazoline) in Comparison to Poly (Ethylene Glycol). *J. Controlled Release* **2016**, *235*, 63−71.
(29) Guillerm, B.; Monge, S.; Lapinte, V.; Robin, J.-J. How to Modulate the Chemical Structure of Polyoxazolines by Appropriate Functionalization. *Macromol. Rapid Commun.* **2012**, *33*, 1600−1612.
(30) Verbraeken, B.; Monnery, B. D.; Lava, K.; Hoogenboom, R. The chemistry of poly(2-oxazoline)s. *Eur. Polym. J.* **2017**, *88*, 451−469.
(31) Bauer, M.; Lautenschlaeger, C.; Kempe, K.; Tauhardt, L.; Schubert, U. S.; Fischer, D. Poly(2-ethyl-2-oxazoline) as Alternative for the Stealth Polymer Poly(ethylene glycol): Comparison of in vitro Cytotoxicity and Hemocompatibility. *Macromol. Biosci.* **2012**, *12*, 986−998.
(32) Li, L.; Yan, B.; Yang, J.; Huang, W.; Chen, L.; Zeng, H. Injectable Self-Healing Hydrogel with Antimicrobial and Antifouling Properties. *ACS Appl. Mater. Interfaces* **2017**, *9*, 9221−9225.
(33) Li, Y.; Pan, T.; Ma, B.; Liu, J.; Sun, J. Healable Antifouling Films Composed of Partially Hydrolyzed Poly(2-Ethyl-2-Oxazoline) and Poly(Acrylic Acid). *ACS Appl. Mater. Interfaces* **2017**, *9* (16), 14429−14436.
(34) Chapman, R.; Bouten, P. J. M.; Hoogenboom, R.; Jolliffe, K. A.; Perrier, S. Thermoresponsive cyclic peptide - poly(2-ethyl-2-oxazoline) conjugate nanotubes. *Chem. Commun.* **2013**, *49*, 6522−6524.
(35) Hendessi, S.; Tatar Güner, P.; Miko, A.; Demirel, A. L. Hydrogen bonded multilayers of poly(2-ethyl-2-oxazoline) stabilized silver nanoparticles and tannic acid. *Eur. Polym. J.* **2017**, *88*, 666−678.
(36) Kempe, K.; Ng, S. L.; Noi, K. F.; Müllner, M.; Gunawan, S. T.; Caruso, F. Clickable Poly(2-oxazoline) Architectures for the Fabrication of Low-Fouling Polymer Capsules. *ACS Macro Lett.* **2013**, *2*, 1069−1072.
(37) Haktaniyan, M.; Atilla, S.; Cagli, E.; Erel-Goktepe, I. pH- and temperature-induced release of doxorubicin from multilayers of poly(2-isopropyl-2-oxazoline) and tannic acid. *Polym. Int.* **2017**, *66*, 1851−1863.
(38) Shutava, T. G.; Lvov, Y. M. Nano-Engineered Microcapsules of Tannic acid and Chitosan for Protein Encapsulation. *J. Nanosci. Nanotechnol.* **2006**, *6*, 1655−1661.
(39) Le Questel, J.-Y.; Laurence, C.; Lachkar, A.; Helbert, M.; Berthelot, M. Hydrogen-Bond Basicity of Secondary and Tertiary Amides, Carbamates, Ureas and Lactams. *J. Chem. Soc. Perkin Transactions 2* **1992**, 2091−2094.
(40) Hoogenboom, R.; Fijten, M. W. M.; Thijs, H. M. L.; van Lankvelt, B. M.; Schubert, U. S. Microwave-assisted synthesis and

DOI: 10.1021/acs.langmuir.9b02938
Langmuir 2019, 35, 14712−14724

properties of a series of poly(2-alkyl-2-oxazoline)s. *Monomers Polym.* **2005**, *8*, 659−671.
(41) Anandhakumar, S.; Nagaraja, V.; Raichur, A. M. Reversible Polyelectrolyte Capsules as Carriers for Protein Delivery. *Colloids Surf., B* **2010**, *78*, 266−274.
(42) Rettler, E. F.-J.; Unger, M. V.; Hoogenboom, R.; Siesler, H. W.; Schubert, U. S. Water Uptake of Poly(2-N-Alkyl-2-Oxazoline)s: Temperature-Dependent Fourier Transform Infrared (FT-IR) Spectroscopy and Two-Dimensional Correlation Analysis (2DCOS). *Appl. Spectrosc.* **2012**, *66*, 1145−1155.
(43) Cagli, E.; Yildirim, E.; Yang, S.-W.; Erel-Goktepe, I. An experimental and computational approach to pH-dependent self-aggregation of poly(2-isopropyl-2-oxazoline). *J. Polym. Sci. B. Polym. Phys.* **2019**, *57*, 210−221.
(44) Karahan, H. E.; Eyüboğlu, L.; Kıyıla, D.; Demirel, A. L. pH-stability and pH-annealing of H-bonded multilayer films prepared by layer-by-layer spin-assembly. *Eur. Polym. J.* **2014**, *56*, 159−167.
(45) Gu, L.; Nusblat, L. M.; Tishbi, N.; Noble, S. C.; Pinson, C. M.; Mintzer, E.; Roth, C. M.; Uhrich, K. E. Cationic amphiphilic macromolecule (CAM)-lipid complexes for efficient siRNA gene silencing. *J. Controlled Release* **2014**, *184*, 28−35.
(46) Shutava, T.; Prouty, M.; Kommireddy, D.; Lvov, Y. pH Responsive Decomposable Layer-by-Layer Nanofilms and Capsules on the Basis of Tannic acid. *Macromolecules* **2005**, *38*, 2850−2858.
(47) Mauser, T.; Déjugnat, C.; Sukhorukov, G. B. Balance of Hydrophobic and Electrostatic Forces in the pH Response of Weak Polyelectrolyte Capsules. *J. Phys. Chem. B* **2006**, *110*, 20246−20253.
(48) Mauser, T.; Déjugnat, C.; Möhwald, H.; Sukhorukov, G. B. Microcapsules made of Weak Polyelectrolytes: Templating and Stimuli-Responsive Properties. *Langmuir* **2006**, *22*, 5888−5893.
(49) Takemoto, Y.; Ajiro, H.; Akashi, M. Hydrogen-Bonded Multilayer Films Based on Poly(N-vinylamide) Derivatives and Tannic Acid. *Langmuir* **2015**, *31*, 6863−6869.

DOI: 10.1021/acs.langmuir.9b02938
Langmuir 2019, 35, 14712−14724